ACS OMEGA

Open Access

http://pubs.acs.org/journal/acsodf

Article

Theoretical Investigation of Thermodynamic Properties of the Al−Si−Fe Ternary Alloy

Wenyuan Hou,* Jiaoru Wang, and Hesong Li*

Cite This: *ACS Omega* 2024, 9, 6316−6324

Read Online

ACCESS | Metrics & More | Article Recommendations

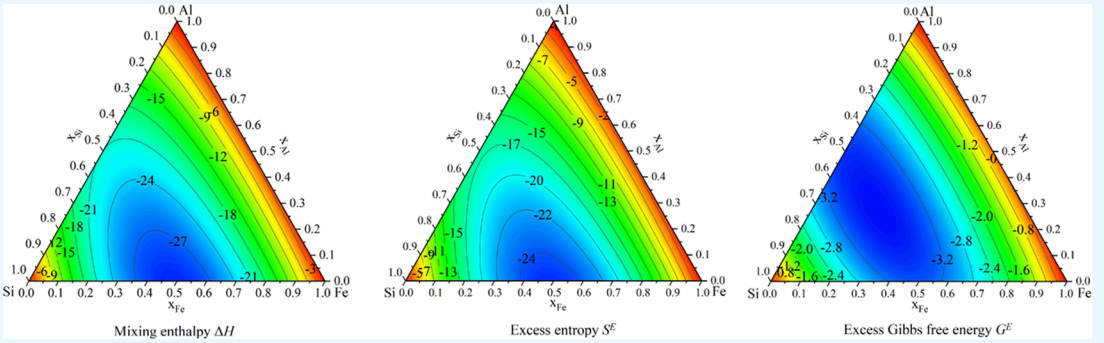

ABSTRACT: Aiming at the current lack of thermodynamic parameters related to the preparation of aluminum−silicon−iron alloys from spent refractory materials in aluminum electrolytic cells, the Miedema model was used to calculate the thermodynamic parameters of Al−Si, Al−Fe, and Si−Fe binary alloys. On this basis, the Toop model was combined to calculate the mixing enthalpy ΔH, excess entropy S^E, excess Gibbs free energy G^E, and component activity α of Al−Si−Fe ternary alloys. The results show that ΔH, S^E, and G^E of binary alloys are all negative values. The properties of the Al element and Si element are similar, and they are different from the Fe element. The ternary alloys also have negative values of ΔH, S^E, and G^E in the alloy composition range, and their values change obviously in the region where the content of Fe is high or low. The activity values of all components decrease dramatically along with the diminishing of the corresponding molar fractions, and the activity values of Al, Si, and Fe are smaller in the central portion of the triangle of ternary components. It indicates that there is a strong interaction between the three elements, which easily forms ternary intermetallic compounds.

1. INTRODUCTION

Spent refractory material is a solid hazardous waste generated during the production of primary aluminum, and its main components are aluminum oxide, silicon oxide, fluoride, and trace cyanide.[1,2] Traditional landfill disposal no longer meets national environmental requirements. How to dispose of spent refractory material has become one of the most important problems to be solved in the electrolytic aluminum industry.[3,4] Our previous work has prepared Al−Si and Al−Si−Fe alloys by adding spent refractory material to aluminum electrolytic cells based on the basic principle of aluminum electrolysis.[5−7] Meanwhile, cyanide with high toxicity could be decomposed in the high-temperature environment of the electrolytic cell, while fluoride could be recycled as a component of the electrolyte. This method could realize harmless treatment and resource utilization of spent refractory material. It is one of the most economical and effective disposal methods at present.

The Al−Si−Fe alloy prepared from spent refractory material has the advantages of high density, low melting point, good wear resistance, good deoxidation effect, etc., which can be widely used in the steelmaking process and also contribute to transportation, aerospace, and other fields.[8−10] The temperature of the melt in the aluminum electrolytic cell is 930−960 °C. However, there are few studies on the thermodynamic properties of the Al−Si−Fe ternary alloy in this temperature range, and the thermodynamic data are scarce at present. Mastering the thermodynamic properties plays an important role in analyzing the relationship between the alloy system and element composition, which can provide guidance for experimental research, industrial production, and practical application of the alloy. Under realistic conditions, the generation of alloy solution is often in a high-temperature environment. It is difficult, costly, and time-consuming to study the thermodynamic properties by experimental methods, and

Received: June 4, 2023
Revised: October 12, 2023
Accepted: January 11, 2024
Published: January 31, 2024

https://doi.org/10.1021/acsomega.3c03921
ACS Omega 2024, 9, 6316−6324

experimental accuracy cannot be guaranteed. Therefore, it is necessary to use a mathematical model combining theory and experience to calculate the thermodynamic data.

The Miedema model has been widely used in the study of the thermodynamic properties of binary alloys due to its simple calculation and high accuracy.[11,12] For ternary alloys, it is mainly based on the thermodynamic properties of binary alloy systems through geometric model extrapolation. Zhang et al.[13] calculated the mixing enthalpy of the Al−Cu−Re ternary alloy system in the whole composition range by using the Miedema theory and the geometric extrapolation model and used it for ternary amorphous composition design and related performance research. Based on the Miedema model and the Toop model, Huang et al.[14] calculated and analyzed the thermodynamic properties of the Mg−Al−Y ternary alloy system. Based on previous studies, calculating the thermodynamic data of the Al−Si−Fe ternary alloy by a mathematical model and analyzing the thermodynamic properties will be helpful to the preparation of the alloy and the resource utilization of the spent refractory material.

Based on the Miedema model and the Toop model, the thermodynamic parameters of Al−Si, Al−Fe, and Si−Fe binary alloys were calculated. On this basis, the mixing enthalpy ΔH, excess entropy S^E, excess Gibbs free energy G^E, and each component activity α of the Al−Si−Fe ternary alloy were calculated and analyzed, which provided theoretical guidance for the preparation and application of the Al−Si−Fe ternary alloy.

2. THERMODYNAMIC PARAMETER CALCULATION MODEL

2.1. Miedema Model. The Miedema model is a semi-empirical model for the mixing enthalpy of transition metal binary compounds based on the Wigner−Seitz model that studies the band structure properties of crystals and the basic physical parameters of elements.[15,16] After a series of deductions and simplifications of the Miedema model, the mixing enthalpy of the binary alloy ΔH_{AB} can be expressed as follows

$$\Delta H_{AB} = f_{AB}\frac{x_A[1+\mu_A x_B(\varphi_A-\varphi_B)]x_B[1+\mu_B x_A(\varphi_B-\varphi_A)]}{x_A V_A^{2/3}[1+\mu_A x_B(\varphi_A-\varphi_B)]+x_B V_B^{2/3}[1+\mu_B x_A(\varphi_B-\varphi_A)]} \quad (1)$$

$$f_{AB} = \frac{2pV_A^{2/3}V_B^{2/3}\{q/p[(n_{ws}^{1/3})_A-(n_{ws}^{1/3})_B]^2-(\varphi_A-\varphi_B)^2-b(r/p)\}}{(n_{ws}^{1/3})_A^{-1}+(n_{ws}^{1/3})_B^{-1}} \quad (2)$$

where x_A and x_B are the mole fractions of alloy components A and B, respectively. V_A and V_B are the molar volumes of components A and B, respectively. φ_A and φ_B are the electronegative parameters of components A and B, respectively. $(n_{WS}^{1/3})_A$ and $(n_{WS}^{1/3})_B$ are the electron densities at the boundary of the Wigner−Seitz cell of components A and B, respectively. μ, p, q, b, and r are the empirical constants.

Table 1. Parameters of Al, Si, and Fe

element	$n_{WS}^{1/3}$	φ/V	$V^{2/3}$/cm^2	μ	T_m/K	r/p	q/p
Al	1.39	4.2	4.6	0.07	933	1.9	9.4
Si	1.50	4.7	4.2	0.04	1683	2.1	9.4
Fe	1.77	4.93	3.7	0.04	1811	1.0	9.4

2.2. Calculation of Component Activity of the Binary Alloy. In the $A-B$ binary alloy system, the relationship between the excess partial molar free energy $\bar{G}_A^E$ and the activity coefficient γ_A of component A is

$$\bar{G}_A^E = RT\ln\gamma_A \quad (3)$$

The excess partial molar free energy $\bar{G}_A^E$ of component A has the following relationship with the excess Gibbs free energy G_{AB}^E in the $A-B$ binary alloy system

$$\bar{G}_A^E = G_{AB}^E + (1-x_A)\frac{\partial G_{AB}^E}{\partial x_A} \quad (4)$$

The relationship of the excess Gibbs free energy G_{AB}^E, excess entropy S_{AB}^E, and mixing enthalpy ΔH_{AB} in the $A-B$ binary alloy system can be expressed as

$$G_{AB}^E = \Delta H_{AB} - TS_{AB}^E \quad (5)$$

The relationship between the mixing enthalpy ΔH_{AB} and excess entropy S_{AB}^E is as follows

$$S_{AB}^E = 0.1\Delta H_{AB}(1/T_{mA}+1/T_{mB}) \quad (6)$$

where T_{mA} and T_{mB} are the melting points of components A and B in the melt, respectively.

Make $\alpha_{AB} = 1-0.1T(1/T_{mA}+1/T_{mB})$, and G_{AB}^E can be expressed as

$$G_{AB}^E = \alpha_{AB}\times\Delta H_{AB} \quad (7)$$

Based on the Miedema model, the relationship between the activity coefficient γ_A of component A and its component fractions x_A can be obtained by combining the above equations as follows

$$\gamma_A = \frac{\alpha_{AB}\Delta H_{AB}(1-x_A)}{RT}\left\{\frac{1}{x_A}-\frac{\mu_A(\varphi_A-\varphi_B)}{1+\mu_A(\varphi_A-\varphi_B)(1-x_A)}+\frac{\mu_B(\varphi_B-\varphi_A)}{1+\mu_B(\varphi_B-\varphi_A)x_A}-\frac{V_A^{2/3}[1+\mu_A(\varphi_A-\varphi_B)(1-2x_A)]+V_B^{2/3}[-1+\mu_B(\varphi_B-\varphi_A)(1-2x_A)]}{x_A V_A^{2/3}[1+\mu_A(\varphi_A-\varphi_B)(1-x_A)]+(1-x_A)V_B^{2/3}[1+\mu_B(\varphi_B-\varphi_A)x_A]}\right\} \quad (8)$$

The activity α_i of each component can be calculated

$$a_i = \gamma_i x_i \quad (9)$$

3. RESULTS AND DISCUSSION

3.1. Calculation of the Thermodynamic Parameters of Al−Si, Al−Fe, and Si−Fe Binary Alloys. The basic physical parameters of Al, Si, and Fe are shown in Table 1.[17] The calculation results of the mixing enthalpy ΔH, excess entropy S^E, excess Gibbs free energy G^E, and component activity α of Al−Si, Al−Fe, and Si−Fe binary alloys are shown in Figure 1. It can be seen that the thermodynamic properties of Al−Fe and Si−Fe binary alloys are close to each other but from those of Al−Si binary alloys. On the whole, ΔH, S^E, and G^E of Al−Si, Al−Fe,

https://doi.org/10.1021/acsomega.3c03921
ACS Omega 2024, 9, 6316−6324

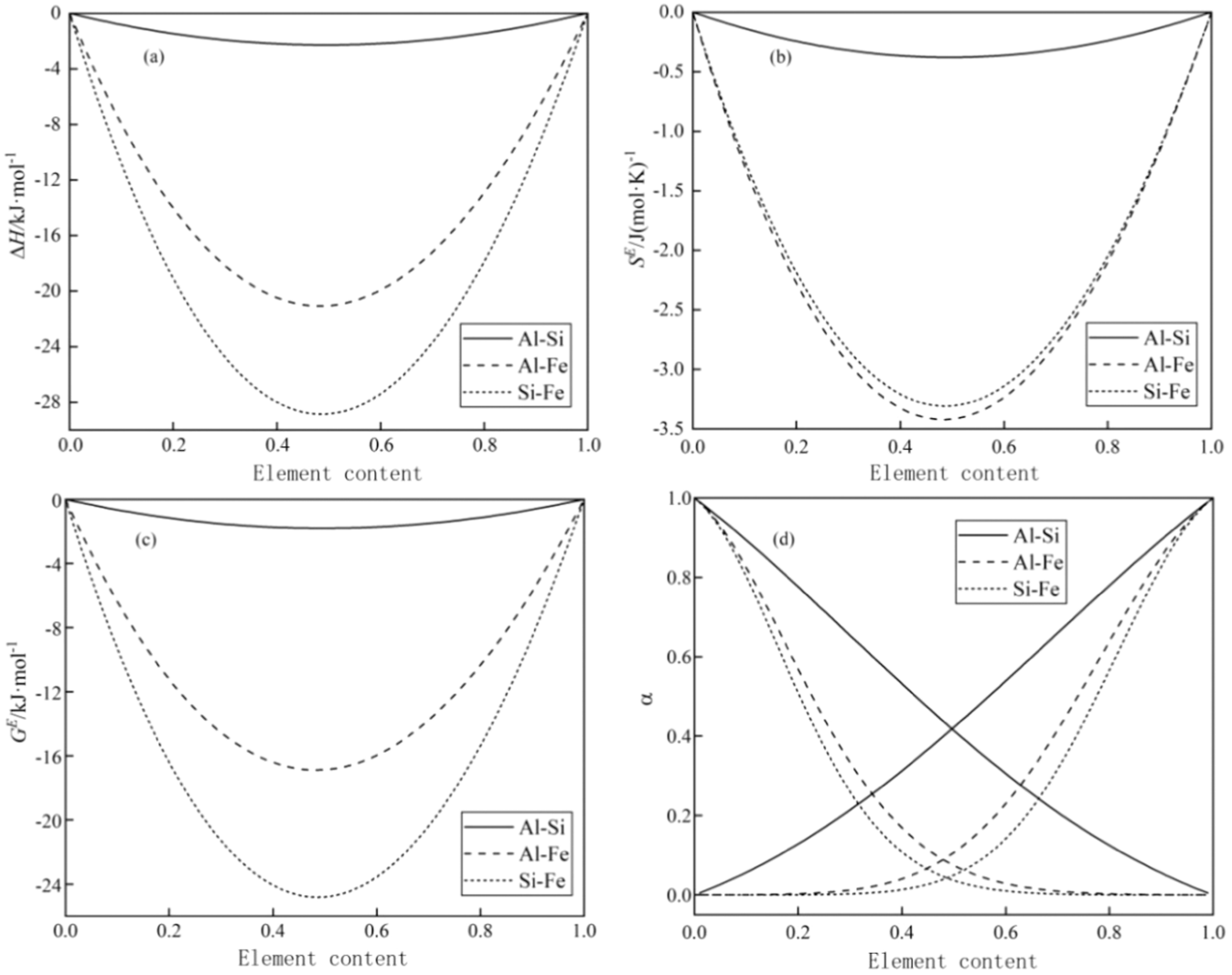

Figure 1. Thermodynamic parameters of Al−Si, Al−Fe, and Si−Fe binary alloys at 1223 K: (a) ΔH; (b) S^E; (c) G^E; and (d) α.

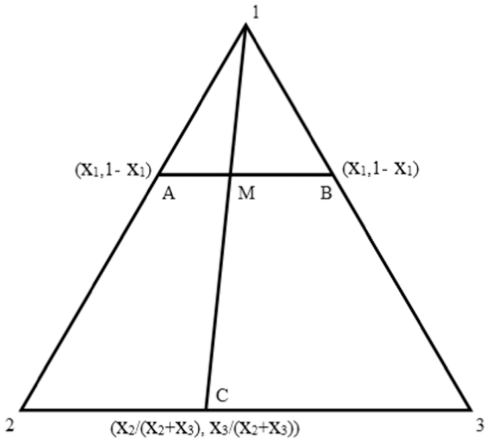

Figure 2. Diagram of component point selection in the binary system for the Toop model.

and Si−Fe binary alloys are all negative, but the absolute values of ΔH, S^E, and G^E of Al−Si binary alloys are much smaller than those of Al−Fe and Si−Fe binary alloys. According to the activity curve of Figure 1(d), it can be seen that the activity of each element in the Al−Si binary alloy is positively correlated to its content, which is close to the ideal solution. However, there are strong negative deviations from Raoult's law in Al−Fe and Si−Fe binary alloys, and the activity curves show obvious concave shapes. The reason for the large difference in activity curves is that the Al and Si elements are the main group elements in the third period with similar atomic numbers and properties, while the Fe element is in the VIIIB group of the fourth period and has very different properties than Al and Si elements. According to the symmetry criterion of the ternary alloy system,[18] the Al−Si−Fe ternary alloy system is an asymmetric system, in which Al and Si are symmetrical components and Fe is an asymmetric component.

Table 2. Composition Ratio of Each Cross Section in the Al−Si−Fe Ternary Alloy System

cross section	*A*	*B*	*C*	*D*	*E*
x_{Al}:x_{Si}	1:9	3:7	5:5	7:3	9:1
x_{Al}:x_{Fe}	1:9	3:7	5:5	7:3	9:1
x_{Si}:x_{Fe}	1:9	3:7	5:5	7:3	9:1

3.2. Calculation of Thermodynamic Parameters of the Al−Si−Fe Ternary Alloy. The properties of ternary systems can be obtained from the properties of binary systems through geometric models. At present, the commonly used geometric

https://doi.org/10.1021/acsomega.3c03921
ACS Omega 2024, 9, 6316−6324

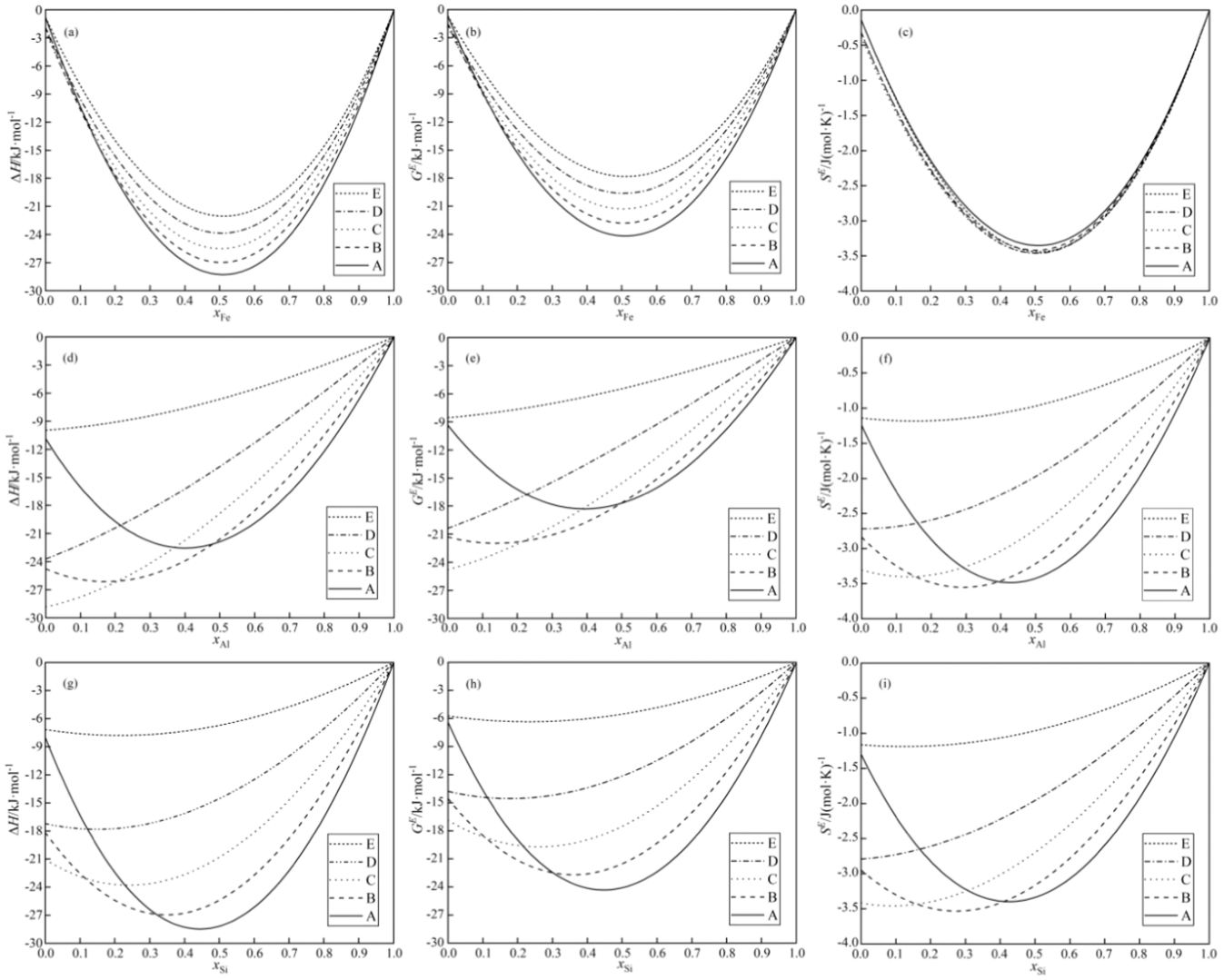

Figure 3. Thermodynamic parameters of the Al−Si−Fe ternary alloy at 1223 K: (a, d, g) ΔH; (b, e, h) G^E; (c, f, i) S^E.

models can be divided into two categories: symmetric models (Kohler model, Muggianu model) and asymmetric models (Toop model, Hillert model).[19,20] Since the asymmetric model takes into account the property differences between components, it has better accuracy than the symmetric model.[18,21] According to the conclusion in the previous section, the properties of Fe are very different from those of Al and Si, and Fe is the asymmetric component. Therefore, using the Toop model for thermodynamic calculation of the Al−Si−Fe ternary alloy can ensure the accuracy of the results. When the Toop model is used to calculate the thermodynamic function, it should be ensured that the mole fraction of the asymmetric component in its binary system is equal to its mole fraction in the ternary alloy system and the mole ratio of the two symmetric components forming a binary system is equal to its mole ratio in the ternary system. The geometric method of point selection for the Toop model is shown in Figure 2.

The equation for the Toop model is as follows

$$X_{ABC}^E = \frac{x_B}{x_B + x_C} X_{AB}^E(x_A, 1 - x_A) + \frac{x_C}{x_B + x_C} X_{AC}^E(x_A, 1 - x_A) + (x_B + x_C)^2 X_{BC}^E\left(\frac{x_B}{x_B + x_C}, \frac{x_C}{x_B + x_C}\right) \quad (10)$$

where X_{ABC}^E, X_{AB}^E, X_{AC}^E, and X_{BC}^E are the excess thermodynamic properties of ternary and binary systems, respectively. x_A, x_B, and x_C are the mole fractions of A, B, and C in the ternary system, respectively.

To study the role and properties of Al, Si, and Fe elements in the whole ternary alloy system, the ratio of the mole fraction of any two elements is fixed, and then the effect of the third element composition on the thermodynamic properties of the ternary alloy system is studied; that is, the vertical cross section of the ternary system through an element point is studied. The composition ratios of each vertical section of the Al−Si−Fe ternary alloy system are shown in Table 2.

The relationship between the mixing enthalpy ΔH, excess entropy S^E, excess Gibbs free energy G^E, and the molar fraction x_i (i = Al, Si, Fe) of the Al−Si−Fe ternary alloy is shown in Figure

https://doi.org/10.1021/acsomega.3c03921
ACS Omega 2024, 9, 6316−6324

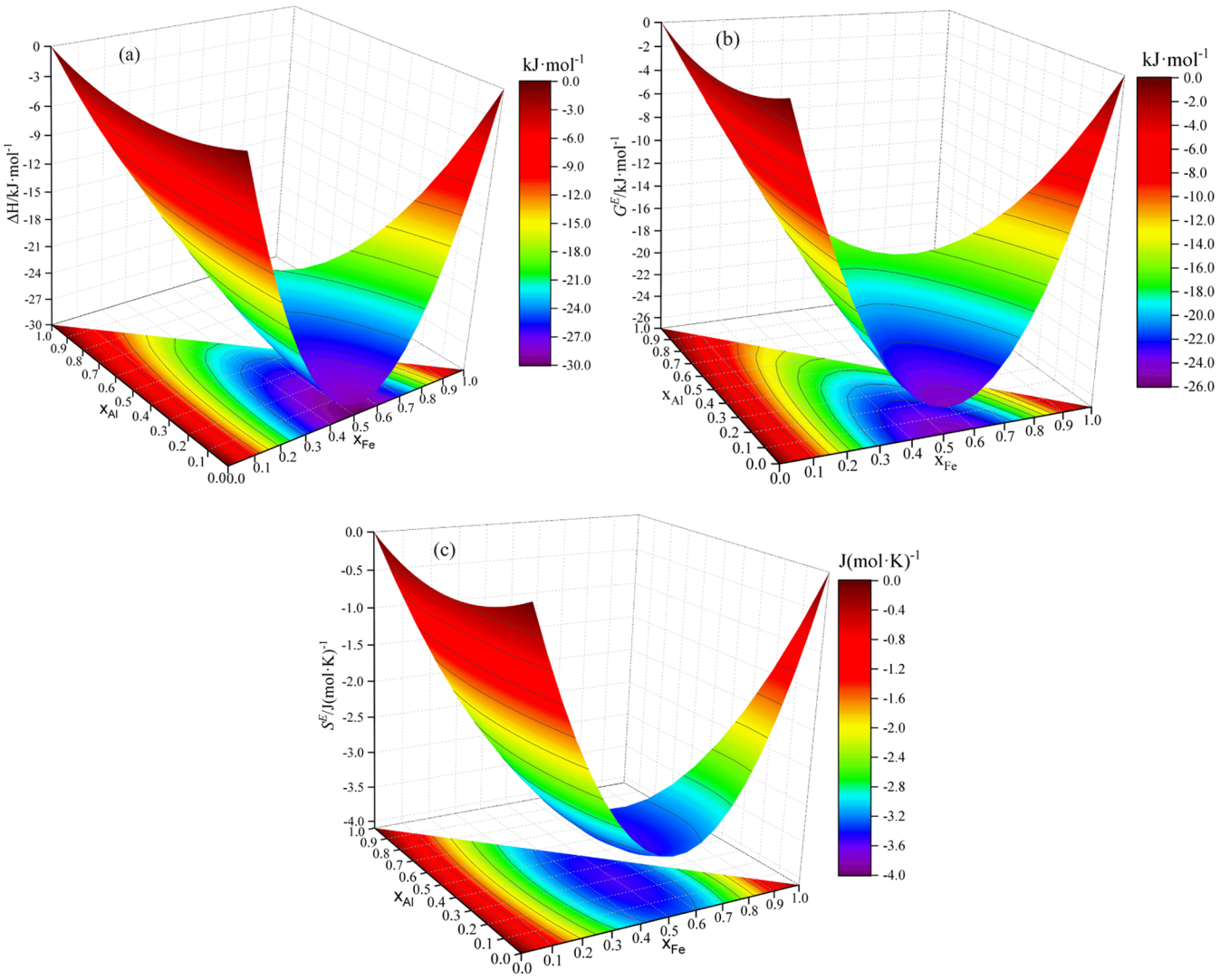

Figure 4. 3D schematic of the thermodynamic parameters of the Al−Si−Fe ternary alloy at 1223 K: (a) ΔH; (b) G^E; and (c) S^E.

3. From Figure 3a−c, it can be seen that the mixing enthalpy, excess entropy, and excess Gibbs free energy of the Al−Si−Fe ternary alloy decrease first and then increase with the increase of the molar fraction of Fe, showing a parabolic shape as a whole. In the cases of *A*, *B*, *C*, *D*, and *E*, five different Al−Si element ratios, the minimum values of the three thermodynamic parameters appear at about the Fe element mole fraction of 0.5.

From Figure 3 d−f, the ΔH, S^E, and G^E of the ternary alloy also show a parabolic shape with the change of the Al mole fraction. However, different Si−Fe ratios have a great influence on the three thermodynamic parameters in the alloy system, especially when the mole fraction of Al is low. The lowest point of most thermodynamic data curves no longer appears at the mole fraction of Al. The main reason is that Fe is an asymmetric component, and its content has a great influence on the thermodynamic parameters of Al−Si−Fe ternary alloys.

It can be seen from Figure 3(g,i) that the thermodynamic parameters still show a parabolic shape with the change of the Si molar fraction, but they are not symmetrical. The overall trend is similar to the change of thermodynamic parameters corresponding to the Al element, which is obviously different from that of the Fe element. It indicates that in the Al−Si−Fe ternary alloy system, the properties of the Al element and the Si element are similar and different from those of the Fe element. It also demonstrates that when the Toop model is used to study the thermodynamic properties of the Al−Si−Fe ternary alloy, it is correct to select the Fe element as the asymmetric component in the ternary alloy system.

Figure 4 shows the three-dimensional diagram of mixing enthalpy, excess free energy, and excess entropy of the Al−Si−Fe ternary alloy at 1223 K. In Figure 4, *x* and *y* coordinates represent the mole fractions of Al and Fe, respectively, while the coordinate information on the component Si is not displayed. The sum of the mole fractions of Al, Si, and Fe in the ternary alloy is 1. Thus, when the mole fractions of Al and Fe are given, the mole fraction of Si is uniquely determined. It can be seen from Figure 4 that the three thermodynamic parameters of the Al−Si−Fe ternary alloy are mainly affected by the change of the mole fraction of the Fe element, showing the characteristics of large values at both ends and small values in the middle.

Although the three-dimensional graph is more intuitive, to facilitate the study, the three-dimensional surface is projected on a plane, and its plane projection is transformed into triangular coordinates. The isolines of mixing enthalpy, excess free energy, and excess entropy of Al−Si−Fe ternary alloy are shown in Figure 5. In Figure 5, ΔH, G^E, and S^E are negative in the range of the ternary alloy composition. When the molar fraction of Fe is between 30 and 70%, the variation trends of ΔH, G^E, and S^E are

https://doi.org/10.1021/acsomega.3c03921
ACS Omega 2024, 9, 6316−6324

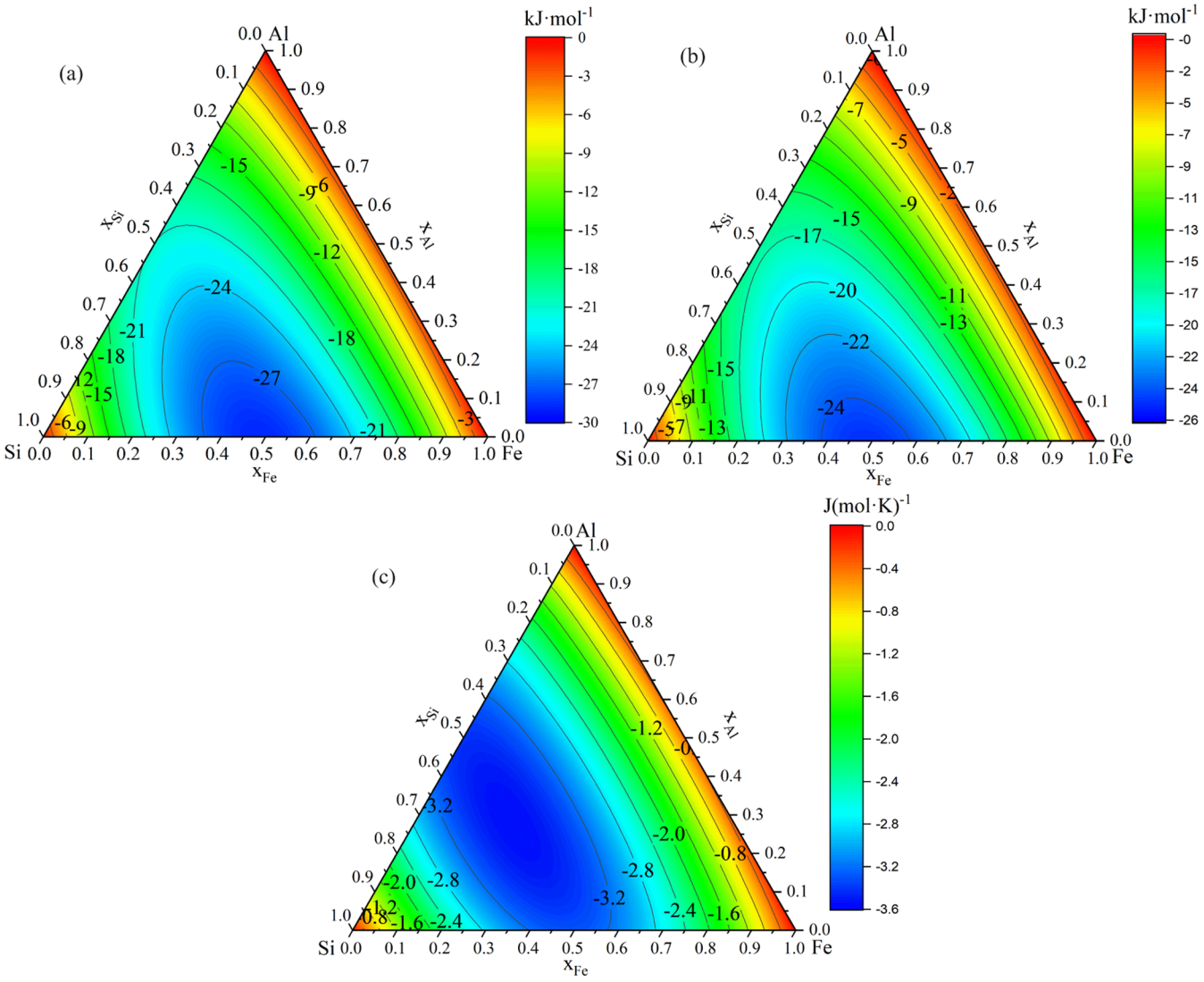

Figure 5. Contour diagram of the thermodynamic parameters of the Al−Si−Fe ternary alloy at 1223 K: (a) ΔH; (b) G^E; and (c) S^E.

relatively gentle. However, in the Fe-rich and Fe-poor regions, the variation trends of ΔH, G^E, and S^E are larger.

The minimum value of S^E appears at the molar fraction ratio of about 0.28:0.32:0.5 (Al:Si:Fe), and its value is −3.544 J mol^{-1} K^{-1}. The minimum values of ΔH and G^E appear at the molar fraction ratio of about 0:0.49:0.51, which are −28.861 and −24.81 kJ mol^{-1}, respectively. The phase composition at the minimum value can be regarded as FeSi, which indicates that the Si element and Fe element may have more affinity than the Al element.

3.3. Activity Calculation of the Al−Si−Fe Ternary Alloy. Activity is a very important part of the thermodynamic properties of ternary alloy systems. In the A−B-C ternary system, there is the following relationship among the excess partial molar free energies

$$\begin{cases} \overline{G}_A^E = G^E - x_B\dfrac{\partial G^E}{\partial x_B} + (1 - x_A)\dfrac{\partial G^E}{\partial x_A} \\ \overline{G}_B^E = G^E - x_A\dfrac{\partial G^E}{\partial x_A} + (1 - x_B)\dfrac{\partial G^E}{\partial x_B} \\ \overline{G}_C^E = G^E - x_A\dfrac{\partial G^E}{\partial x_A} - x_B\dfrac{\partial G^E}{\partial x_B} \end{cases} \tag{11}$$

where G_i^E is the excess partial molar free energy of component i (i = A, B, C) in the A−B−C ternary alloy. G^E is the excess free energy of the A−B−C ternary alloy.

G^E is expressed by eq 10, which can be simplified into an equation concerning x_A and x_B. Substituting G^E into eq 11 for derivative calculation, $\overline{G}_A^E$, $\overline{G}_B^E$, and $\overline{G}_C^E$ can be obtained. According to eqs 3 and 9, the activity of each component of the Al−Si−Fe ternary alloy can be calculated. For more detailed calculation steps, please refer to ref 22. The three-dimensional relationship between the activity and the alloy content is shown in Figure 6. It can be seen that the activity trends of the Al element and the Si element are very similar, and the activities of both elements are very small at a low mole fraction. When the

https://doi.org/10.1021/acsomega.3c03921
ACS Omega 2024, 9, 6316−6324

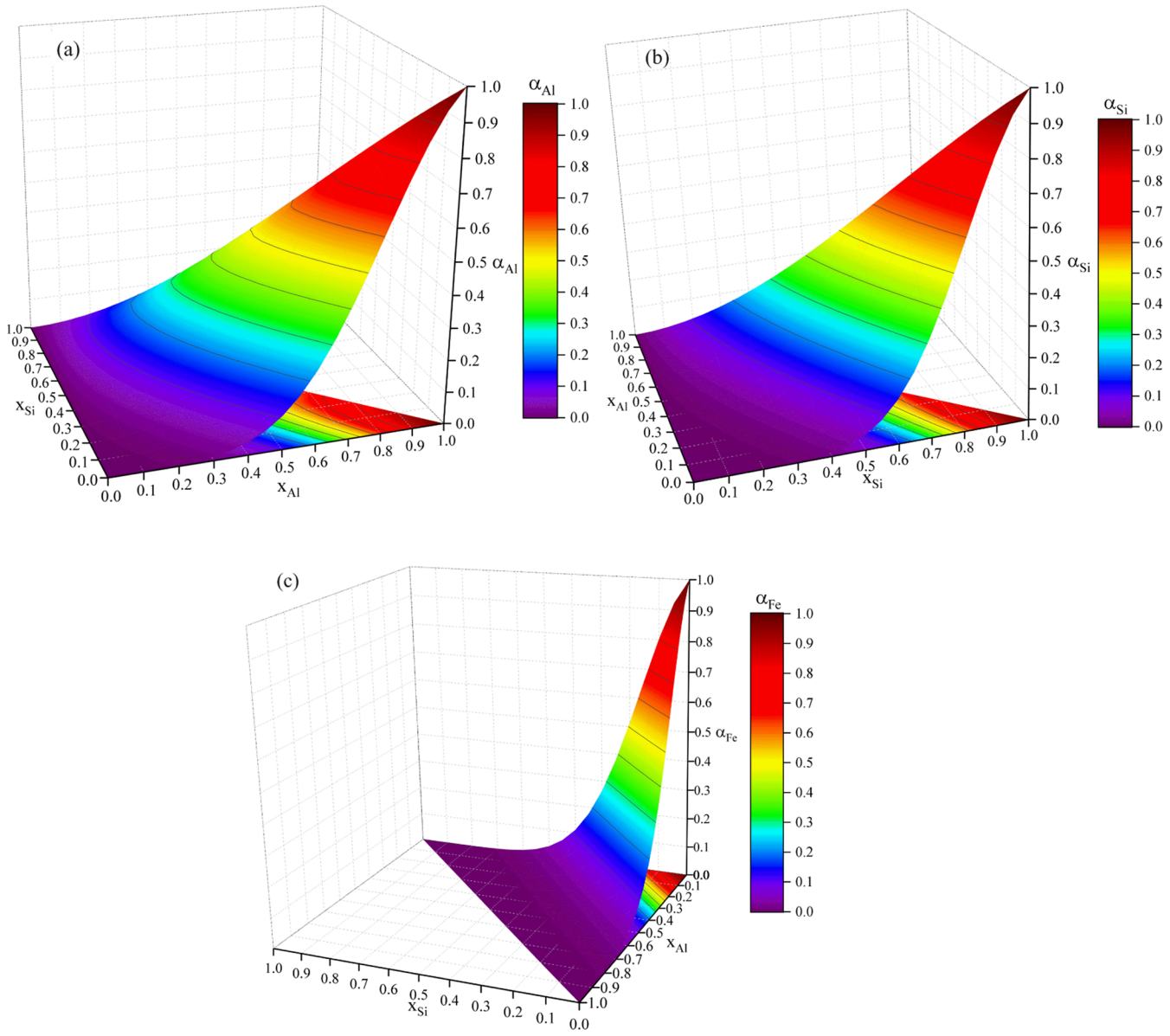

Figure 6. 3D diagram of the activity for each group of Al−Si−Fe ternary alloy at 1223 K: (a) α_{Al}; (b) α_{Si}; and (c) α_{Fe}.

molar fraction of the Al element or the Si element is larger than 0.5, the corresponding activity increases faster.

Referring to the processing method of thermodynamic parameters of the ternary alloy system, the three-dimensional stereogram of activity is projected on the plane, and the contour map of the activity of each component is shown in Figure 7. From Figure 7, it can be seen that the isolines of the activity of each component in the Al−Si−Fe ternary alloys are mostly concentrated in the enrichment area of the corresponding element, indicating that the smaller the molar fraction of the element in the ternary alloy, the smaller the corresponding activity value of the element. With the decrease of the molar fraction of the element, the corresponding activity value decreases sharply. In addition, at the center of the coordinate triangle, the activity values of each component are small, indicating that there is a strong interaction between the three elements, and it is easy to form ternary intermetallic compounds.

4. CONCLUSIONS

The properties of the Al element and the Si element in the Al−Si−Fe ternary alloy system are similar and are obviously different from the Fe element. It is reasonable to select the Fe element as an asymmetric component in the thermodynamic study of the Al−Si−Fe ternary alloy by the Toop model.

The mixing enthalpy ΔH, excess free energy G^E, and excess entropy S^E of the ternary alloy are negative in the range of alloy compositions. The variation gradient of the three thermodynamic parameters is larger in the Fe-rich and Fe-poor regions. When the Fe content is between 30% and 70%, the variation gradient of the three thermodynamic parameters is relatively gentle.

The minimum value of S^E at 1233 K is obtained at x_{Al} = 28%, x_{Si} = 32%, and x_{Fe} = 50%, and its value is −3.544 J mol^{-1} K^{-1}. The minimum values of ΔH and G^E are obtained at x_{Al} = 0%, x_{Si} = 49%, and x_{Fe} = 51%, which are −28.861 and −24.81 kJ mol^{-1}, respectively. The phase composition at the minimum value can

https://doi.org/10.1021/acsomega.3c03921
ACS Omega 2024, 9, 6316−6324

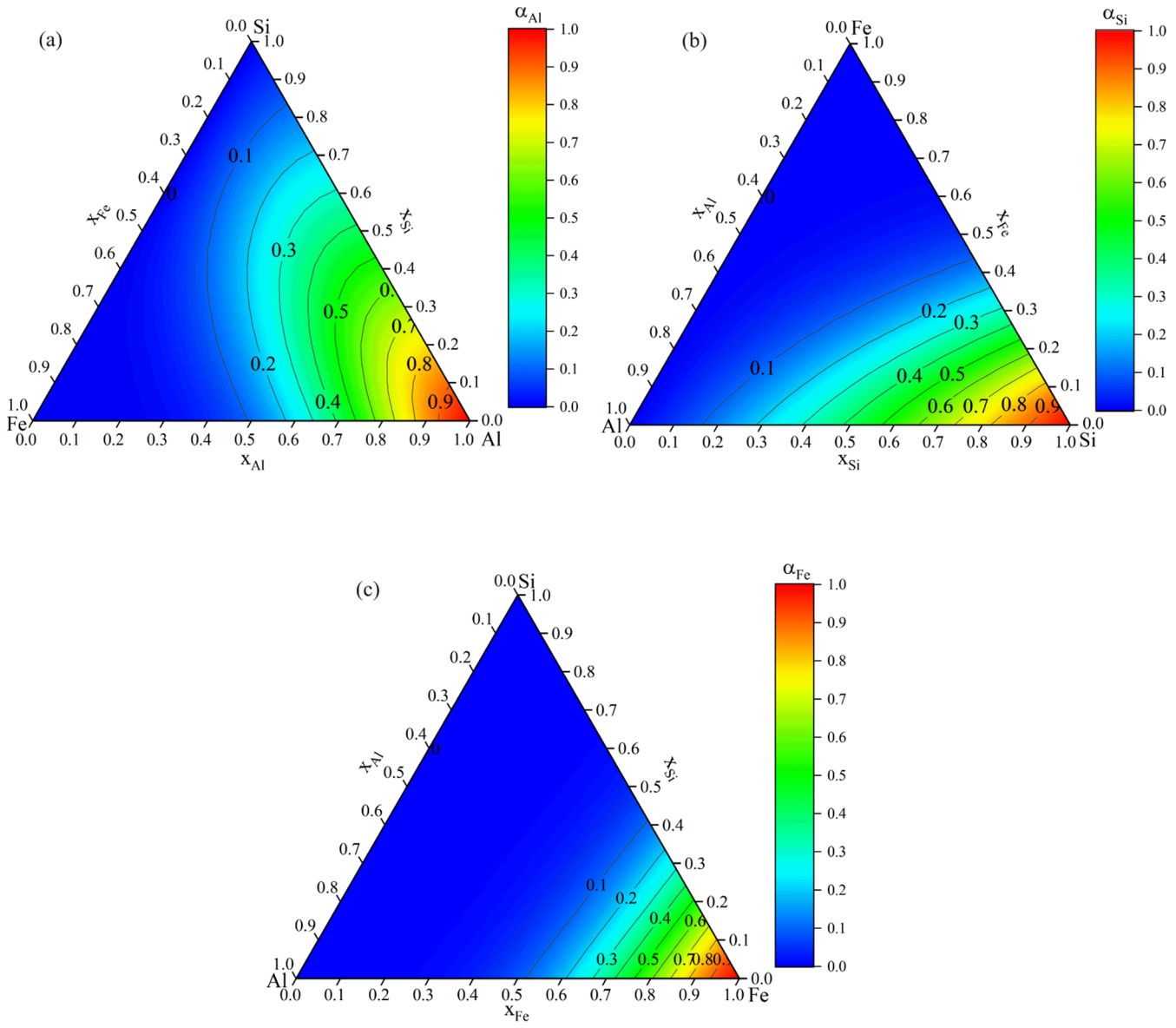

Figure 7. Contour diagram of the activity for each group of Al−Si−Fe ternary alloy at 1223 K: (a) α_{Al}; (b) α_{Si}; and (c) α_{Fe}.

be regarded as FeSi, which indicates that the Si and Fe elements may have more affinity than the Al element.

AUTHOR INFORMATION

Corresponding Authors

Wenyuan Hou − *School of Energy and Power Engineering, North University of China, Taiyuan 030051, China;* orcid.org/0000-0002-5362-6678; Email: zndxhwy@163.com

Hesong Li − *School of Energy Science and Engineering, Central South University, Changsha 410083, China;* Email: lihesong@csu.edu.cn

Author

Jiaoru Wang − *School of Energy Science and Engineering, Central South University, Changsha 410083, China*

Complete contact information is available at: https://pubs.acs.org/10.1021/acsomega.3c03921

Notes

The authors declare no competing financial interest.

ACKNOWLEDGMENTS

This research was supported by the Fundamental Research Program of Shanxi Province (202203021222028) and the Fundamental Research Funds for the Central Universities of Central South University (2018zzts157). The authors also thank the anonymous referees for valuable comments and useful suggestions that helped us to improve the quality of our present and future work.

REFERENCES

(1) Tu, H.; Li, X.; Muhammad, Y.; Jin, X.; Lin, H.; Pei, R.; Zhao, Z.; Li, J. Feasibility of reuse of modified electrolytic aluminium spent refractory material in asphalt and assessment of its environmental stability. *J. Cleaner Prod.* **2023**, *389*, No. 136072.

(2) Hou, W. Theoretical and Application Study on Co-Processing Spent Refractory Materials in the Aluminum Reduction Cell, Ph.D. Dissertation; Central South University: China, 2021.

(3) Ospina, G.; Hassan, M. I. Spent pot lining characterization framework. *JOM* **2017**, *69*, 1639−1645.
(4) Li, S.; Liu, W.; Yang, G.; Kang, Z.; Liu, Z. Present situation of treatment technology of spent pot lining aluminum electrolysis. *Inorg. Chem. Ind.* **2020**, *52*, 6−10.
(5) Li, H.; Hou, W.; Cui, T. A method for treating aluminum silicate solid waste in waste lining of aluminum electrolytic cell. China Patent, CN111005038, 2021.
(6) Li, H.; Hou, W.; Xu, T. A preparation method of aluminum-silicon-iron alloy. China Patent, CN109913911, 2019.
(7) Hou, W.; Li, H.; Li, M.; Cheng, B. Recycling of spent refractory materials to produce Al-Si master alloys via the aluminum reduction cell. *J. Cleaner Prod.* **2021**, *289*, No. 125162.
(8) Qi, M.; Kang, Y.; Li, J.; Shang, B. Improvement in mechanical, thermal conductivity and corrosion performances of a new high-thermally conductive Al-Si-Fe alloy through a novel R-HPDC process. *J. Mater. Process. Technol.* **2020**, *279*, No. 116586.
(9) Kim, J.; Jang, G. S.; Kim, M. S.; Lee, J. K. Microstructure and compressive deformation of hypereutectic Al-Si-Fe based P/M alloys fabricated by spark plasma sintering. *Trans. Nonferrous Met. Soc. China* **2014**, *24*, 2346−2351.
(10) Zou, X.; Yan, H. Thermodynamic and kinetic analysis of ternary intermetallics formation in Al−Cu−La alloy. *Phys. B* **2022**, *646*, No. 414254.
(11) Li, H.; Lu, X.; Bin, J.; Wei, D.; Gao, Z. Calculation of thermodynamic properties of Al-Zr, Al-Y and Zr-Y binary alloy melts. *J. Cent. South Univ.* **2013**, *44*, 1806−1812.
(12) Boom, R.; Boer, F. R. Enthalpy of formation of binary solid and liquid Mg alloys - Comparison of Miedema-mode calculations with data reported in literature. *Calphad* **2020**, *68*, No. 101647, DOI: 10.1016/j.calphad.2019.101647.
(13) Zhang, L.; Wang, R.; Tao, X.; Ouyang, Y. Thermodynamic properties of Al-Cu-RE ternary alloys calculated with Miedema's theory. *Rare Met. Mater. Eng.* **2015**, *44*, 628−633.
(14) Huang, W.; Yan, H. Calculation of thermodynamic parameters of Mg-Al-Y Alloy. *J. Wuhan Univ. Technol.* **2014**, *29*, 374−378.
(15) Miedema, A. R. *Theory of Alloy Phase Formation*; The Metallurgical Society of AIME: New York, 1980.
(16) Alsaedi, A. K.; Ivanova, A. G.; Habieb, A. A.; Almayahi, B. A. Estimation of the functions of some iron-based ternary systems within Miedema model and comparison with experiment. *Results Phys.* **2020**, *16*, No. 102969.
(17) Miedema, A. R.; de Chatel, P. F.; de Boer, E. R. Cohesion in alloys-fundamentals of a semi-empirical model. *Phys. B+C* **1980**, *100*, 1−28, DOI: 10.1016/0378-4363(80)90054-6.
(18) Luo, Q.; Li, Q.; Zhang, J. Y.; Chou, K. C. Comparison of Muggianu model, Toop model and General solution model for predicting the thermodynamic properties of Mg-Al-Zn system. *Calphad* **2015**, *51*, 366.
(19) Ouyang, Y.; Zhong, X.; Du, Y.; Feng, Y.; He, Y. Enthalpies of formation for the Al−Cu−Ni−Zr quaternary alloys calculated via a combined approach of geometric model and Miedema theory. *J. Alloys Compd.* **2006**, *420*, 175−181.
(20) Sun, S.; Yi, D.; Zang, B. Calculation of thermodynamic parameters of Al-Si-Er alloy based on Miedema model and Toop model. *Rare Met. Mater. Eng.* **2010**, *39*, 1974−1978.
(21) Tang, Y.; Huang, C.; Ding, S.; Huang, F.; Tu, J.; Wang, Y.; Zhong, M. Theoretical calculation of surface tension of Ag-Au-Cu alloy. *Chin. J. Nonferrous Met.* **2020**, *30*, 595−603.
(22) Li, R. Q. The application of R function to new asymmetric model and toop model. *Calphad* **1989**, *13*, 67−70, DOI: 10.1016/0364-5916(89)90040-0.

https://doi.org/10.1021/acsomega.3c03921
ACS Omega 2024, 9, 6316−6324